

Sequential Contrastive Audio-Visual Learning

Ioannis Tsiamas^{1*†}, Santiago Pascual², Chunghsin Yeh², Joan Serra²

¹ Universitat Politècnica de Catalunya, Barcelona

² Dolby Laboratories

Abstract

Contrastive learning has emerged as a powerful technique in audio-visual representation learning, leveraging the natural co-occurrence of audio and visual modalities in extensive web-scale video datasets to achieve significant advancements. However, conventional contrastive audio-visual learning methodologies often rely on aggregated representations derived through temporal aggregation, which neglects the intrinsic sequential nature of the data. This oversight raises concerns regarding the ability of standard approaches to capture and utilize fine-grained information within sequences, information that is vital for distinguishing between semantically similar yet distinct examples. In response to this limitation, we propose sequential contrastive audio-visual learning (SCAV), which contrasts examples based on their non-aggregated representation space using sequential distances. Retrieval experiments with the VGGSound and Music datasets demonstrate the effectiveness of SCAV, showing 2–3× relative improvements against traditional aggregation-based contrastive learning and other methods from the literature. We also show that models trained with SCAV exhibit a high degree of flexibility regarding the metric employed for retrieval, allowing them to operate on a spectrum of efficiency-accuracy trade-offs, potentially making them applicable in multiple scenarios, from small- to large-scale retrieval.

1 Introduction

Audio-visual representation learning is at the core of several recent advancements such as multimodal LLMs (Zhang, Li, and Bing 2023; Gemini-Team 2023) and generative models used in video-to-audio (Luo et al. 2023), audio-to-video (Jeong et al. 2023), joint audio-visual (Ruan et al. 2023), and any-to-any (Tang et al. 2023) synthesis. Contrastive learning (Chopra, Hadsell, and LeCun 2005; van den Oord, Li, and Vinyals 2019), which aims to distinguish between similar and dissimilar pairs of data points, has emerged as an effective methodology for learning audio-visual representations by relying on the co-occurrence of the two modalities in unlabeled web-scale video datasets (Korbar, Tran, and Torresani 2018; Ma et al. 2021a). The stan-

*Corresponding author at ioannis.tsiamas@upc.edu

†Work done while at Dolby Laboratories.

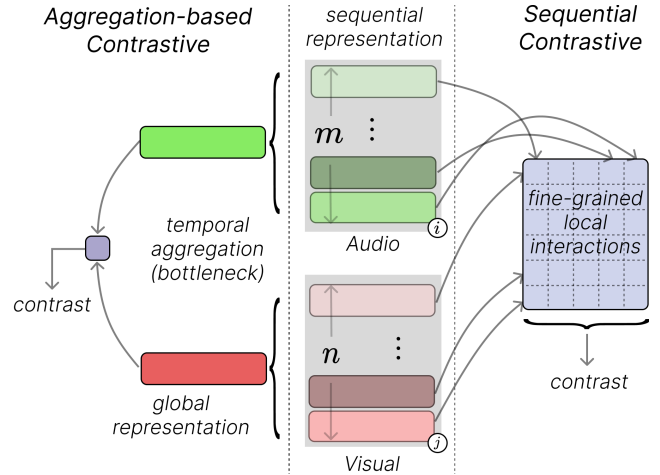


Figure 1: Aggregation-based vs. our proposed sequential-based contrastive strategy.

standard approach for contrastive audio-visual learning (CAV) is to contrast between global embedding vectors, which should ideally capture all the semantics of each example. In the case of audio and video, such vectors are typically obtained by aggregating the sequence of feature vectors, either by mean aggregation (Wu et al. 2023b; Xu et al. 2021; Gong et al. 2023) or by using a learnable `<cls>` token (Wu et al. 2023a). A simplified example of this process is presented in the left part of Fig. 1.

Although a global embedding might be sufficient for static modalities, like images (Radford et al. 2021), we argue that it is potentially over-compressing for modalities of a dynamic nature, like videos or music, thus hindering the effectiveness of contrastive learning and the robustness of the multimodal space. Consider the challenge of audio-visual retrieval in the context of music videos, where the goal is to find video segments that closely match a given audio query, such as a snippet of melody or rhythm. Traditional methods, which rely on globally aggregated vectors, may struggle due to the dynamic and complex nature of music videos. For example, a user might search for video segments that feature a particular guitar riff accompanied by a dynamic stage performance. If the sequential nature of the representations has

been lost due to compressing into a single aggregated vector, key details about the guitar’s tone, the riff’s tempo, and the corresponding visual elements (e.g., the guitarist’s movements, lighting changes, etc.) could be lost. A more nuanced approach that maintains the temporal and expressive details of both audio and video modalities could dramatically improve retrieval accuracy in such cases.

In this paper, we propose sequential contrastive audio-visual (SCAV) learning, which operates directly on natural and non-aggregated representation spaces, and can thus take advantage of the fine-grained local semantic information available in the feature sequences (Fig. 1). Our proposed method aims to obtain a robust sequential and multimodal representation space that can be useful for several tasks, such as generation or retrieval. In the retrieval scenario, we experiment with different sequential distance metrics for the proposed SCAV method, considering both accuracy and efficiency. Interestingly, after training single-modality encoders to contrastively align feature sequences, we find that a simple Euclidean distance is more effective, efficient, and scales better to larger batch sizes than complex functions such as Dynamic Time Warping (Vintsyuk 1968) or Wasserstein (Frogner et al. 2015) distances. Using sequence-based retrieval, our proposed contrastive method with the Euclidean formulation surpasses its aggregation-based counterpart by a large margin. SCAV also outperforms other state-of-the-art methods from the literature like ImageBind (Girdhar et al. 2023) and CAV-MAE (Gong et al. 2023), which are both larger and pretrained on more data. Furthermore, the gap becomes more evident for zero-shot retrieval on the challenging Music dataset (Zhao et al. 2018), which demands for high capabilities of intra-sequence modeling and discrimination. Finally, we take advantage of an emergent property of our models, which allows them to use either the efficient aggregation-based retrieval or the more accurate sequence-based one. Thus, we additionally propose a hybrid approach that combines the best of both strategies and provides a flexible trade-off between accuracy and efficiency.

2 Background

2.1 Related Works

Contrastive learning has been traditionally used in self-supervised unimodal representation learning such as vision pretraining (Chen et al. 2020b) and audio pretraining (Baevski et al. 2020). Recently it has also achieved impressive results in multimodal representation learning, by utilizing large amounts of (weakly) supervised data. Examples can be found in vision-language (Radford et al. 2021; Jia et al. 2021) and audio-language (Wu et al. 2023b; Elizalde, Deshmukh, and Wang 2023) modalities, and recently also when dealing with more than two modalities (Girdhar et al. 2023; Guzhov et al. 2022; Wang et al. 2023; Cheng et al. 2023).

The general correspondence of the audio and visual modalities in the natural world has led to the application of contrastive learning in audio-visual representation learning through unlabeled web-scale video datasets. Early works

used this audio-visual correspondence in a discriminative approach, either predicting whether a visual and an audio frame originate from the same point in the video (Arandjelovic and Zisserman 2017; Arandjelovic and Zisserman 2018) or focusing on the temporal synchronicity between visual and audio clips (Owens and Efros 2018; Korbar, Tran, and Torresani 2018). A fully-contrastive framework was later adopted (Morgado, Vasconcelos, and Misra 2021), while further works proposed to improve the quality of negative examples (Ma et al. 2021a; Kalayeh et al. 2022) and to target the issues of false positives and false negatives in the contrastive framework (Morgado, Misra, and Vasconcelos 2021; Sun et al. 2023). Some works used both local and global information to enhance the generalisability of the learned representations (Ma et al. 2021b; Recasens et al. 2021). More recently, MAViL (Huang et al. 2023) and CAV-MAE (Gong et al. 2023) combine the contrastive task with mask data modeling, which improves the quality of the audio-visual representations. Similar to these works, we also make use of contrastive learning. However, in different than these works, we formulate it in a sequential distance setting, making better use of the rich and fine-grained temporal information of audio and video representations.

For video-paragraph pretraining, TempCLR (Yang et al. 2023) proposed to generate negative examples by shuffling the order of clips and sentences in the video, and applied contrastive learning with dynamic time wrapping (DTW) (Vintsyuk 1968) as a sequential distance metric. In the context of mobile robotics and the task of visual place recognition, SeqMatchNet (Garg, Vankadari, and Milford 2021) first encodes visual frames in sequential representations and then applies contrastive learning with a triplet loss based on euclidean distances, which improves visual recall. To the best of our knowledge, these two are the only works that have used sequential distances in a contrastive learning framework. However, none of them deals with audio-visual representations. In our work, we further consider several different sequential distances which we investigate in terms of both accuracy and compute. Furthermore, we also apply the sequential distances for retrieval at inference time with drastically improved performance, and propose a hybrid retrieval approach that is as accurate and also computationally cheaper than sequence-based retrieval.

2.2 Aggregation-based Contrastive Learning

We now describe how standard (aggregation-based) contrastive learning is performed (Morgado, Vasconcelos, and Misra 2021; Ma et al. 2021a). In this and the following sections, we denote tensors and matrices with uppercase bold (\mathbf{X}), vectors and columns of such matrices with lowercase bold (\mathbf{x}), and single numbers or elements of such matrices or vectors with regular italics (x, X). Given a batch of B visual and audio representations $\{(\mathbf{H}^{v_i}, \mathbf{H}^{a_i})\}_{i=1}^B$ extracted from videos, where $\mathbf{H}^{v_i} \in \mathbb{R}^{n_i \times c}$ and $\mathbf{H}^{a_i} \in \mathbb{R}^{m_i \times c}$ represent row-wise sequences of n_i and m_i feature vectors of dimensionality c , respectively, the aggregation-based audio-visual contrastive loss is defined as

$$\mathcal{L}^{\text{agg}} = -\frac{1}{2B} \sum_{i=1}^B \left[\log \left(\frac{\exp(s_{ii}/\tau)}{\sum_{j=1}^B \exp(s_{ij}/\tau)} \right) + \log \left(\frac{\exp(s_{ii}/\tau)}{\sum_{j=1}^B \exp(s_{ji}/\tau)} \right) \right], \quad (1)$$

where $\tau > 0$ is a learnable temperature parameter and s_{ij} is the cosine similarity between temporally-aggregated video and audio representations:

$$s_{ij} = \frac{(\bar{\mathbf{h}}^{v_i})^\top \cdot \bar{\mathbf{h}}^{a_j}}{\|\bar{\mathbf{h}}^{v_i}\|_2 \cdot \|\bar{\mathbf{h}}^{a_j}\|_2}. \quad (2)$$

Temporal aggregation is performed by row-wise averaging \mathbf{H} such that $\bar{\mathbf{h}} \in \mathbb{R}^c$, thus allowing for $n_i \neq m_i$. Note that indices i and j switch the order in the second term of the summation in Eq. 1, and that such indices are not associated with video or audio but with the element in the batch. The goal of Eq. 1 is to pull together the aggregated audio and visual representations that originate from the same example and, at the same time, push away the ones originating from different ones.

A caveat of this approach is that it disregards the sequential nature of the visual and audio modalities, since it is applied on aggregated representations $\bar{\mathbf{h}}$. Although Eq. 2 can match the general semantics through these representations, it is doubtful whether it can adequately model the relations between different temporal sub-spaces within them. Take, for example, a visual scene where three events are happening in order, as in $(\epsilon_1^v, \epsilon_2^v, \epsilon_3^v)$, and two semantically similar, but temporally different audio scenes $(\epsilon_1^a, \epsilon_2^a, \epsilon_3^a)$ and $(\epsilon_3^a, \epsilon_2^a, \epsilon_1^a)$. Eqs. 1, 2 provide the correct signal to the model as to which representations to pull/push, but the bottlenecked mean-aggregated space potentially does not have the capacity to do so, even though we use a quite complex model to produce \mathbf{H} . Thus, it becomes questionable whether the vanilla formulation of contrastive learning can accurately learn how to disambiguate between the correct and false audio-visual pairings in such scenarios, which are not so rare in web-scale video datasets.

3 Method

The model we consider is depicted in Fig. 2. It consists of a visual and an audio processing stack. We first extract pre-trained features for each modality using frozen visual and audio front-end models, and then further process them with learnable Transformer blocks, to obtain audio-visual sequential semantic representations. In the following sections, we provide a detailed overview of the model architecture (Sec. 3.1), followed by our proposed sequence-based formulation (Sec. 3.2), with several different possible distance functions. Finally, we discuss the ways in which the trained models can be used for audio-visual retrieval and propose a sequence-based and a hybrid methodology (Sec. 3.3).

3.1 Architecture

Given an unlabelled video, which we denote with subindex i , we extract the visual and audio sequences $\mathbf{V}^i, \mathbf{A}^i$, where

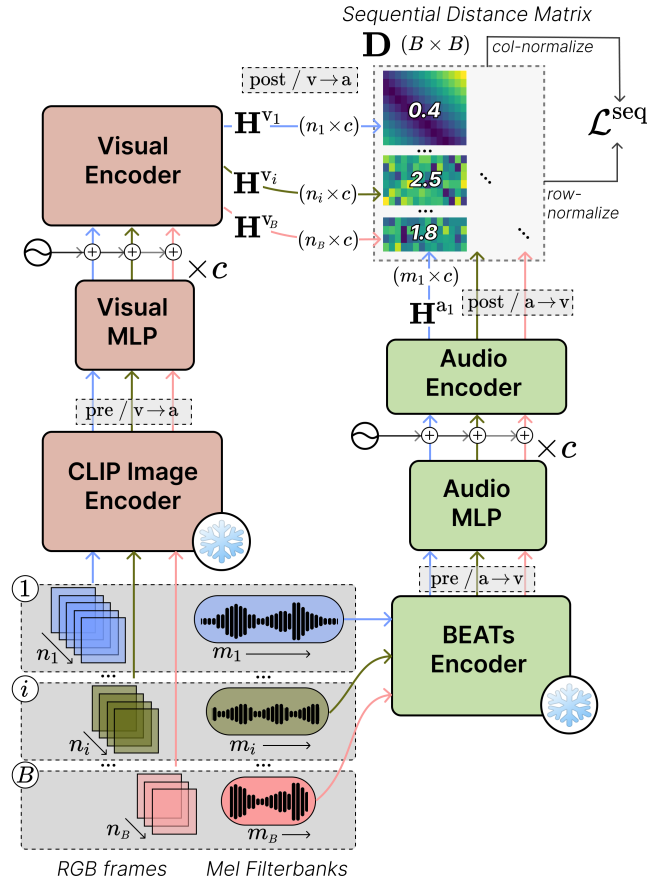


Figure 2: Model Architecture for Sequential Contrastive Learning (SCAV)

$\mathbf{V}^i \in \mathbb{R}^{n_i \times h \times w \times 3}$ is a sequence of n_i visual frames and $\mathbf{A}^i \in \mathbb{R}^{m_i \times b}$ is a sequence of m_i audio frames containing Mel filterbank features. Note that the two sequences can have different sampling rates and thus, in general, $n_i \neq m_i$. Using \mathbf{V}^i and \mathbf{A}^i , we obtain visual and audio features via pre-trained models CLIP (Radford et al. 2021) and BEATs (Chen et al. 2023). We use the pre-trained encoders as feature extractors, and thus keep them frozen during training.

CLIP is a vision-language model that has been pre-trained with contrastive learning on a large dataset of paired images and textual descriptions. It thus serves as a state-of-the-art visual recognition front-end, and furthermore its multimodal nature can allow for our framework to be extended to the text modality in the future. We use the image encoder from CLIP, which is a Vision-Transformer (ViT) (Dosovitskiy et al. 2021). We process each frame separately and then concatenate them to obtain a sequence of semantic visual representations, expressed as $\hat{\mathbf{V}}^i$.

BEATs is a state-of-the-art audio tagger that has been pre-trained with self-supervised learning and finetuned on large-scale audio event classification. Different from other audio front-ends that are limited to providing a single semantic representation for the whole audio (Wu et al. 2023b;

Elizalde, Deshmukh, and Wang 2023), outputs from BEATs are fine-grained per-frame predictions of audio events. This can provide us with a semantically-rich sequential audio representation that can be beneficial in cases where multiple sequential events are happening within an audio. We use the encoder of BEATs that also follows the ViT architecture¹. We discard the linear classification layer and thus use the final hidden representation of the encoder, thus obtaining a sequence of semantic audio features, expressed as the matrix $\hat{\mathbf{A}}^i$.

We first project both $\hat{\mathbf{V}}^i$ and $\hat{\mathbf{A}}^i$ to the same dimensionality c using two-layered MLPs. Next, we employ two randomly initialized encoders to obtain the latent matrix representations $\mathbf{H}^{v_i} \in \mathbb{R}^{n_i \times c}$ and $\mathbf{H}^{a_i} \in \mathbb{R}^{m_i \times c}$. The two encoders follow a Transformer architecture with c channels and sinusoidal positional encodings (Vaswani et al. 2017). The number of blocks for the two encoders will vary (4.1), as the audio representation is already a well-formed sequence and thus requires a less complex processing than the visual one, which comes from independently extracted frame representations. In summary, we perform:

$$\begin{aligned}\mathbf{H}^{v_i} &= \text{enc}^v \left(\text{mlp}^v(\hat{\mathbf{V}}^i) + \beta^v \cdot \text{pos}(n_i) \right), \\ \mathbf{H}^{a_i} &= \text{enc}^a \left(\text{mlp}^a(\hat{\mathbf{A}}^i) + \beta^a \cdot \text{pos}(m_i) \right),\end{aligned}$$

where, $\text{pos}(\cdot)$ is the positional encoding function for relative positional embeddings (Chi et al. 2022) and $\beta^v, \beta^a > 0$ are learnable parameters. Although BEATs has positional information through relative positional embeddings (Chen et al. 2023), we found it beneficial to re-introduce them with $\text{pos}(\cdot)$.

3.2 Sequential Contrastive Learning

Unlike previous works which use aggregation-based contrastive learning, here we compute a distance directly on the sequential latent representations (without any compression/pooling), and thus propose the following contrastive loss:

$$\mathcal{L}^{\text{seq}} = -\frac{1}{2B} \sum_{i=1}^B \left[\log \left(\frac{\exp(-\bar{d}_{ii}^{\text{row}}/\tau^{\text{seq}})}{\sum_{j=1}^B \exp(-\bar{d}_{ij}^{\text{row}}/\tau^{\text{seq}})} \right) + \log \left(\frac{\exp(-\bar{d}_{ii}^{\text{col}}/\tau^{\text{seq}})}{\sum_{j=1}^B \exp(-\bar{d}_{ji}^{\text{col}}/\tau^{\text{seq}})} \right) \right], \quad (3)$$

where $\tau^{\text{seq}} > 0$ is a learnable temperature hyperparameter and $d_{ij} \geq 0$ is the result of a distance function between visual and audio representation sequences \mathbf{H}^{v_i} and \mathbf{H}^{a_j} , $d_{ij} = \text{dist}(\mathbf{H}^{v_i}, \mathbf{H}^{a_j})$. We consider three different sequential distance functions for $\text{dist}(\cdot)$, which we analyze in the following subsections. We denote the matrix of $B \times B$ pairwise distances by \mathbf{D} .

It is important to note that, for each of the two terms in Eq. 3, we shift and re-scale \mathbf{D} by row- and column-wise z-score normalization. This is crucial in order to signify the

¹The input Mel Filterbank features are patchified and the output is de-patchified again to a monotonically aligned sequence, see (Chen et al. 2023).

differences between correct and in-correct pairs, which diminish due to the distance being computed in a very high-dimensional space $(n_i \times c) \times (m_j \times c)$. Specifically, we use

$$\bar{\mathbf{D}}^{\text{row}} = \frac{\mathbf{D} - \text{mean}_{\text{row}}(\mathbf{D})}{\text{std}_{\text{row}}(\mathbf{D})} \quad (4)$$

$$\bar{\mathbf{D}}^{\text{col}} = \frac{\mathbf{D} - \text{mean}_{\text{col}}(\mathbf{D})}{\text{std}_{\text{col}}(\mathbf{D})}. \quad (5)$$

Interpolated Euclidean Since two audio-visual sequences have in general different sampling rates ($n_i \neq m_j$), a straightforward method to get a sequential distance measure is to interpolate² one of the sequences to the length of the other one, and then calculate the mean squared euclidean distance between every corresponding point in the sequences. There are several options for the interpolation, regarding the direction of interpolation, from visual to audio ($v \rightarrow a$) or from audio to visual ($a \rightarrow v$) resolutions, and regarding the application level, which can be at the pre-trained features (pre, using \mathbf{V}, \mathbf{A}) or at the shared representation space (post, using $\mathbf{H}^v, \mathbf{H}^a$) (also denoted in Fig. 2). More formally,

$$\begin{aligned}\text{dist}_{v \rightarrow a}^{\text{Eucl}}(\mathbf{H}^{v_i}, \mathbf{H}^{a_j}) &= \frac{1}{m_j} \sum_{k=1}^{m_j} \delta(\mathbf{h}_k^{v_i \rightarrow a_j}, \mathbf{h}_k^{a_j}), \\ \text{dist}_{a \rightarrow v}^{\text{Eucl}}(\mathbf{H}^{v_i}, \mathbf{H}^{a_j}) &= \frac{1}{n_i} \sum_{k=1}^{n_i} \delta(\mathbf{h}_k^{v_i}, \mathbf{h}_k^{a_j \rightarrow v_i}),\end{aligned} \quad (6)$$

where $\delta: \mathbb{R}^c \times \mathbb{R}^c \rightarrow \mathbb{R}_+$ is the squared euclidean distance between two normalized c -dimensional vectors,

$$\delta(\mathbf{x}, \mathbf{y}) = \sum_{i=1}^c \left(\frac{\mathbf{x}_i}{\|\mathbf{x}\|_2} - \frac{\mathbf{y}_i}{\|\mathbf{y}\|_2} \right)^2, \quad (7)$$

and $\mathbf{h}_k^{v \rightarrow a} \in \mathbb{R}^{m_j \times c}$ and $\mathbf{h}_k^{a \rightarrow v} \in \mathbb{R}^{n_i \times c}$ are the interpolated sequences. We experiment with all these options regarding the direction ($v \rightarrow a/a \rightarrow v$) and the level (pre/post) of the interpolation, considering both performance and compute.

Dynamic Time Warping DTW (Vintsyuk 1968; Itakura 1975) is defined as the distance associated with the shortest alignment path between the two sequences, where the two sequences can have different lengths. Since DTW is not differentiable, we are using its differentiable variant soft-DTW (Cuturi and Blondel 2017), which is defined as

$$\text{dist}^{\text{DTW}}(\mathbf{H}^{v_i}, \mathbf{H}^{a_j}) = \min_{\gamma} \sum_{(k,l) \in \pi} \delta(\mathbf{h}_k^{v_i}, \mathbf{h}_l^{a_j}), \quad (8)$$

where δ is the squared euclidean distance (Eq. 7), π denotes the set of all possible alignment paths, and \min^{γ} represents the soft-minimum operator influenced by the hyperparameter $\gamma > 0$ ($\gamma \rightarrow 0$ yields an approximation increasingly close to the original DTW distance).

²The term interpolation applies to both up-sampling and down-sampling sequences.

Wasserstein Finally, we examine the application of the Wasserstein distance (Frognier et al. 2015) using optimal transport (Peyré and Cuturi 2019). Assuming two uniform probability distributions χ^i, ψ^j , with $\chi_k^i = 1/n_i$ and $\psi_l^j = 1/m_j$, that define the mass in each position of the visual and audio representations, and given a pairwise squared euclidean cost matrix $\Delta^{ij} \in \mathbb{R}_+^{n_i \times m_j}$, where $\Delta_{kl}^{ij} = \delta(\mathbf{h}_k^{v_i}, \mathbf{h}_l^{a_j})$, the Wasserstein distance is defined as the minimum transportation cost over all possible transportation plans $\mathbf{Z}^{ij} \in \mathbb{R}_+^{n_i \times m_j}$ between the two representations. To make it differentiable and efficient to compute we are using the upper-bound regularized version and evaluate it with the Sinkhorn algorithm (Knopp and Sinkhorn 1967):

$$\begin{aligned} \text{dist}^{\text{WASS}}(\mathbf{H}^{v_i}, \mathbf{H}^{a_j}) = \\ \min_{\mathbf{Z}^{ij}} \left(\sum_{(k,l) \in \pi} \mathbf{Z}_{kl}^{ij} \cdot \delta(\mathbf{h}_k^{v_i}, \mathbf{h}_l^{a_j}) - \xi \cdot H(\mathbf{Z}^{ij}) \right) \quad (9) \\ \text{s.t.} \quad \sum_{l=1}^{m_j} \mathbf{Z}_{:,l}^{ij} = 1/n_i \quad \text{and} \quad \sum_{k=1}^{n_i} \mathbf{Z}_{k,:}^{ij} = 1/m_j, \end{aligned}$$

where $\xi > 0$ is a hyperparameter and $H(\cdot)$ the Von Neuman entropy of a matrix.

Since the Wasserstein distance is permutation invariant, and thus by default is a distance measure between two sets of points, to make it sequential, we concatenate two positional regularization terms $\nu^i \in \mathbb{R}^{n_i}$ and $\mu^j \in \mathbb{R}^{m_j}$ in order to penalize the transportation of mass between two distant points (Le et al. 2023; Tsiamas et al. 2024). Thus, the Wasserstein distance (Eq. 9) is applied using the modified representations $\bar{\mathbf{H}}^{v_i} \in \mathbb{R}^{n_i \times (c+1)}$ and $\bar{\mathbf{H}}^{a_j} \in \mathbb{R}^{m_j \times (c+1)}$:

$$\bar{\mathbf{H}}^{v_i} = [\mathbf{H}^{v_i}; \lambda \nu^i], \quad \text{where} \quad \nu_k^i = \frac{k-1}{n_i-1}, \quad (10)$$

and

$$\bar{\mathbf{H}}^{a_j} = [\mathbf{H}^{a_j}; \lambda \mu^j], \quad \text{where} \quad \mu_l^j = \frac{l-1}{m_j-1}, \quad (11)$$

using $\lambda > 0$ as a positional regularization hyperparameter.

3.3 Retrieval with Sequential Distances

Aggregation-based Retrieval To use the trained model for audio-visual cross-modal retrieval, we can apply (row-wise) mean-aggregation to the representations $\mathbf{H}^{v_j}, \mathbf{H}^{a_j}$ to obtain collapsed (temporally-aggregated) c -dimensional embeddings for the whole test set. Then, when querying with the i -th visual embedding, we retrieve the index j^* of the audio embedding with the highest cosine similarity score (Eq. 2). In section 4.2 we will see that, despite being trained on a sequence basis, SCAV can also perform retrieval with aggregated embeddings.

Sequence-based Retrieval The use of sequential contrastive learning during training can enable the application of sequential distances also for retrieval. Thus, querying with the representation i , we retrieve the audio representation j^* with the lowest sequential distance dist . Here, dist is

either the interpolated Euclidean, the DTW³, or the Wasserstein distance, depending on which function was used during training. Also note that we do not have to apply the z-score normalization applied during training (Eq. 4), since it is a monotonic transformation.

Hybrid Retrieval Since sequence-based retrieval can be computationally expensive for large-scale scenarios, we also propose a hybrid, filtering-based approach for retrieval. This approach works by first doing a pre-selection of the k most similar candidates (with k significantly lower than the size of the test set) by leveraging the relatively cheap aggregation-based retrieval, and then performing the final selection by employing the more computationally-demanding sequence-based retrieval on the pre-selected pool of k candidates.

4 Experiments

4.1 Setup

Data We use the data from VGGSound dataset (Chen et al. 2020a) to train and test our models, which contains 10-second clips from YouTube videos. For training we use 153,000 videos (we use a sample of 550 videos from the training set for validation), and for testing we use 13,000 videos from the test split.⁴ For out-of-distribution testing we use the test split of the Music dataset (Zhao et al. 2018; Zhao et al. 2019). The nature of these videos requires strong audio onset detection from the close-up camera recording of someone playing a musical instrument, therefore we use this dataset to evaluate retrieval in a challenging setting. We extracted 1,908 test video clips, each spanning 10 s duration, from a non-overlapped sliding window applied upon 103 test videos effectively downloaded from the MUSIC21-solo test partition.⁵

Model Architecture For each video, we extract its RGB visual frames at its native sampling rate (usually 30 fps, which amounts to a sequence of length 300 for a 10-second video). Each frame is processed independently with a visual front-end, which is a CLIP image encoder: we use the ViT-B/32 configuration, which is based on the Vision-Transformer (Dosovitskiy et al. 2021), with 12 blocks, dimensionality of 768 and 12 attention heads, with a total of 90 M parameters.⁶ The input to the model is divided into patches of 32×32 of pixels and flattened. At the output, the `<cls>` token is used as the representation of the image/frame, which is projected to a dimensionality of 512.

For the audio stream of each video, we resample to 16 kHz and extract 128-dimensional Mel Filterbank features with a window of 25 ms. Mel Filterbank sequences are processed by the BEATs encoder (Chen et al. 2023), which has been pretrained with self-supervised learning and then fine-tuned on audio classification with AudioSet-2M (Gemmeke et al.

³For retrieval we can use actual DTW instead of its differentiable version.

⁴Our train/test splits have less data than the original VGGSound due to missing videos and to filtering videos with low quality and videos without sound.

⁵github.com/roudimit/MUSIC_dataset

⁶huggingface.co/openai/clip-vit-base-patch32

2017).⁷ BEATs is a Transformer with 12 blocks and dimensionality of 768, and has in total 90M parameters. We remove the audio classification head and use the final hidden representation. The input to BEATs is split into 16×16 patches and flattened. Its output is reconstructed to a monotonic sequence by stacking the patches of each time-step along the feature dimension, resulting in an output dimensionality of 6144. It has a resolution of 6.2 fps and thus a 10-second audio has length of 62. CLIP and BEATs networks remain frozen in all our experiments.

The visual and audio MLPs of our model have hidden dimensions of 2048 and 768 respectively, and project to a common dimensionality of 512. The scale of the positional encodings is learned and initialized to $1/\sqrt{512}$. The visual and audio Transformers have 8 and 2 blocks, respectively, both with a dimensionality of 512, hidden dimension of 2048, 8 attention heads, and pre-layernorm (Xiong et al. 2020). The GELU activation function (Hendrycks and Gimpel 2023) is used in the MLPs and the Transformers. The total number of training parameters for our model is 38M.

Training Details We use AdamW (Loshchilov and Hutter 2019) ($\beta_1=0.95$, $\beta_2=0.98$) with a base learning rate of $7 \cdot 10^{-4}$ and a cosine scheduler with linear warm-up (see below). All models are trained with one loss function, either the standard aggregation-based one (Eq. 1), which we denote as CAV, or the sequence-based one (Eq. 3), which we denote as SCAV. The sequence-based one can be based on the interpolated euclidean (Eq. 6, the DTW (Eq. 8, or the Wasserstein (Eq. 9). Experiments with smaller batch sizes (less than 100 examples) are trained for 250k steps with 10k warm-up, while experiments with larger ones are trained for 150k steps with 5k warm-up. Dropout is set to 0.1 for all modules. When training with the aggregation-based contrastive loss (Eq. 1), we mean-aggregate the representations to individual 512-dimensional embeddings and initialize the learnable temperature to $\tau = 0.07$, as in (Radford et al. 2021; Wu et al. 2018). When training with the sequence-based contrastive loss (Eq. 3), we found it useful to initialize the temperature to $\tau^{\text{seq}} = 1$. For the soft-DTW we tune γ to 1 (Eq. 8), while for the Wasserstein distance we use $\xi = 1$ for the entropy regularization (Eq. 9) and tune λ to 1 for the positional regularization (Eqs. 10,11). Our models are trained on an NVIDIA V100-32GB using full precision.

Evaluation We average the 10 best checkpoints according to validation set performance. We evaluate on the test sets of VGGSound and Music using either aggregation-based or sequence-based retrieval (section 3.3), and report Audio-to-Visual ($A \rightarrow V$) and Visual-to-Audio ($V \rightarrow A$) Recall measured at 1 and 5. In the last part of the results, we perform hybrid retrieval and a small ablation.

4.2 Results

CAV/SCAV Variants We first investigate the effectiveness of the proposed SCAV learning on bidirectional retrieval in VGGSound-Test. In the left part of Table 1, we

present the Recall at 1 (R@1) in a setting where we trained with small batch sizes of 32 examples (section 4.1) and using a single contrastive objective (aggregation-based or sequence-based). We observe that SCAV models can benefit dramatically by using sequence-based retrieval instead of the standard aggregation-based one (Agg vs. Seq). Furthermore, among the sequential distances, the interpolated Euclidean outperforms soft-DTW and Wasserstein, while also being simpler and more efficient. We hypothesize that, when using Euclidean distances for training, the Transformer blocks learn to smooth out some warping invariances, if needed. Lastly, we notice that even though models trained with the SCAV objective have not been explicitly optimized to perform aggregation-based retrieval, they can do fairly well in a zero-shot fashion, being competitive with the CAV models (Agg columns).

The batch size is a special hyperparameter in contrastive learning, since usually the higher the better, as the contrastive signal becomes more certain with more negatives. Thus, in order to make a more fair comparison, assuming the same computational budget for all methods, we repeat the experiments but with maxing-out the batch size (max BS, right part of Table 1). Note that, due to the computations required for the pairwise sequential distance matrices (Eq. 3), most methods cannot scale beyond a batch size of 64 in a 32 GB GPU.⁸ We observe that the SCAV configuration where we apply pre-interpolation from video-to-audio (Eucl/pre/v \rightarrow a), when fully scaled to a batch size of 256, can surpass the other methods⁹. This indicates that, at least for VGGSound, a higher resolution in the representations is not that crucial, and it can be traded-off in favor of more negatives in the batch. For a fair comparison, we also perform the same pre interpolation for the CAV method, which can then be scaled to 1024 examples per batch. Interestingly, we do not notice any improvement, which is possibly explained by diminishing returns in the effect of more negatives per aggregated example. Due to its simplicity, scalability, and performance, we focus the rest of the experimentation on SCAV with interpolated Euclidean.

Comparison with Other Methods In Table 2 we provide the results of our method in VGGSound-Test and also in the zero-shot and out-of-distribution data of the Music-Test dataset. We compare against two strong baselines from the literature¹⁰: ImageBind (Girdhar et al. 2023), which added other modalities to the CLIP space, having around 1B parameters, and CAV-MAE (Gong et al. 2023) which was trained with masked data modeling and aggregation-based contrastive learning using AudioSet-2M (Gemmeke et al. 2017), a superset of VGGSound. In VGGSound, we observe that SCAV can surpass the previously proposed methods

⁸We use vectorized operations to efficiently obtain the corresponding distance matrices. One could increase the batch size beyond these numbers by iterative computations, but these would increase dramatically the training time.

⁹For an example of 10 seconds, the audio sequence has a length of 62 due to BEATs’ resolution, so most batches are down-sampled to this number in pre/v \rightarrow a.

¹⁰We re-run the provided public models for our test splits.

⁷github.com/microsoft/unilm/tree/master/beats
Fine-tuned BEATs_iter3+ (AS2M) (cpt2)

Contrastive Method	BS	R@1				max BS	R@1			
		A → V		V → A			A → V		V → A	
		Agg	Seq	Agg	Seq		Agg	Seq	Agg	Seq
CAV	32	10.2	10.6	10.3	8.0	192	12.2	12.7	12.5	11.6
CAV _{pre/v → a}	32	10.0	10.6	9.7	7.9	1024	12.1	12.2	12.1	11.6
SCAV _{Eucl/pre/v → a}	32	8.7	18.7	7.6	18.3	256	11.9	22.6	10.1	22.3
SCAV _{Eucl/pre/a → v}	32	9.0	18.6	8.1	18.3	64	9.7	20.8	8.3	20.5
SCAV _{Eucl/post/v → a}	32	9.5	19.2	8.2	18.4	96	11.4	21.3	7.8	21.3
SCAV _{Eucl/post/a → v}	32	9.3	18.6	7.7	18.4	64	10.0	20.6	7.5	20.1
SCAV _{DTW}	32	9.2	12.5	9.8	13.0	64	9.5	14.2	11.5	15.9
SCAV _{Wasserstein}	32	11.1	15.0	9.5	14.8	64	11.3	16.1	9.7	16.6

Table 1: Bidirectional retrieval results (R@1) in VGGSound-Test with different contrastive methods. Models are run with either the aggregation-based contrastive objective (CAV) or the sequence-based one (SCAV). Each model is run with a small batch size (BS) of 32, and a maxed-out batch size (max BS). For each model, we perform aggregation-based retrieval (Agg) and sequence-based retrieval with the corresponding distance used in SCAV training (Seq). CAV models use the interpolated Euclidean for sequence-based retrieval. The subscript in the method name indicates the interpolation used, if any (pre/post and v → a/a → v).

by large margins, indicating that it can make better use of the fine-grained sequential information in the audio-visual representations. More specifically, it improves R@1 by 10–12 points compared to ImageBind, and 14–15 points compared to CAV-MAE. It is noteworthy that our aggregation-based contrastive method (CAV) is competitive with previous works, which we hypothesize is due to the use of BEATs as an audio front-end (sequence-based, non-aggregated features).

In Music, for which all models are evaluated zero-shot, SCAV outperforms again previous works and CAV, by even larger margins in relative comparisons. More specifically, the post-interpolation Euclidean contrastive variant is more than 3 times better than ImageBind and CAV-MAE in terms of R@1. The Music dataset is not only out-of-distribution due to its domain, but also much more challenging due to the presence of multiple videos with almost identical visual and acoustic features. Thus, the higher performance of our proposed method in this challenging setting re-enforces our claim for the importance of a representation space with proper intra-sequence temporal modeling. Finally, we find that different variants of SCAV score better for each dataset. This is because the post/a → v is expansive and can thus provide more sequential contrastiveness (crucial for Music), as compared to pre/v → a, which is compressive and can use more negatives within a batch (better for VGGSound).

Hybrid Retrieval Although the benefits of retrieval with sequential distances compared to mean aggregation and cosine similarity are evident, there is an extra computational overhead. This overhead is not an issue when performing retrieval in VGGSound, but it can become problematic in large-scale retrieval settings of millions of examples. This can work for models trained with sequential contrastive learning due to their emergent aggregation-based retrieval capabilities (Table 1, Agg columns). In Figure 3 we test this hypothesis with a range of values for k in both VGGSound and Music. The results suggest that hybrid retrieval can

achieve the upper-bound Recall score of the full sequence-based retrieval with $k = 100$. This showcases a useful flexibility in the trade-off between efficiency and accuracy, which is not present in models trained with aggregation-based contrastive learning. Table 3 shows a speed test with the hybrid retrieval approach. We test, for different values of k , the time to retrieve 1,000 queries in a test set of 10,000 candidates ($k = 10^0$ means aggregation-based retrieval, while $k = 10^4$ is the full sequence-based retrieval). Results indicate that, although sequence-based can be costly, the hybrid approach is indeed efficient. At $k = 10^2$, where according to Fig. 3 we already reach the retrieval score of the sequence-based approach, the hybrid approach has only a $\times 1.5$ and $\times 1.8$ computational overhead compared to the aggregation-based one.

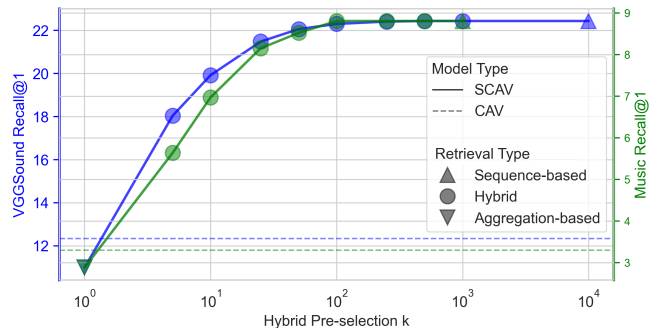


Figure 3: Hybrid Retrieval on VGGSound test (left y-axis) and Music test (right y-axis). Recall@1 is the average of A → V and V → A scores. x-axis has log scale.

Ablations We conclude with three ablations, presented at Table 4. We find that shifting and re-scaling with z-score normalization is essential for our method, since without it, performance is almost on par with aggregation-based contrastive learning. This is likely due to the sequential dis-

Models	Training parameters	VGGSound				Music			
		A → V		V → A		A → V		V → A	
		R@1	R@5	R@1	R@5	R@1	R@5	R@1	R@5
ImageBind _{HUGE}	1 B	10.8	26.4	12.1	28.6	2.5	12.2	2.6	11.4
CAV-MAE _{scale+}	200 M	5.5	14.0	6.5	17.1	2.3	9.6	2.1	10.0
CAV	38 M	12.2	31.1	12.5	30.8	3.8	10.5	2.8	11.5
SCAV _{Eucl/pre/v→a} [†]	38 M	22.6	42.7	22.3	42.3	9.3	21.8	7.3	19.4
SCAV _{Eucl/post/a→v} [†]	38 M	21.3	42.0	21.3	40.9	9.5	22.5	8.1	21.3

Table 2: Bidirectional retrieval results in VGGSound and Music (Zero-shot) test. Upper part of the Table is other works, and lower part is this work. All methods are evaluated on the same test sets. † use Sequence-based retrieval.

k	GPU	CPU
10^0	0.33 ($\times 1.0$)	2.6 ($\times 1.0$)
10^1	0.38 ($\times 1.2$)	3.6 ($\times 1.4$)
10^2	0.50 ($\times 1.5$)	4.6 ($\times 1.8$)
10^3	1.73 ($\times 5.2$)	7 ($\times 28.0$)
10^4	13.90 ($\times 42.0$)	741.0 ($\times 285.0$)

Table 3: Absolute (in seconds) and relative inference time for hybrid retrieval of 1 k queries in a test set of 10 k candidates.

Method	A → V	V → A
SCAV _{Eucl/pre/v→a}	22.6	22.3
↔ w/o Dist. Norm.	12.5	12.7
↔ w/ Small τ^{seq} Init.	18.6	18.5
↔ w/ multi-tasking	15.3	15.4

Table 4: Ablations. Bidirectional retrieval with Recall@1 in VGGSound-Test.

tances being not very distinct from each other due to the high-dimensional space, which is eased by the normalization. Furthermore, contrary to the standard way of initializing the temperature with small values (e.g., 0.07 in (Wu et al. 2018; Radford et al. 2021)), in our sequential setting is better to start training from a larger value (e.g., 1). This entails that the task is harder in the start of the training, due to the scaled logits in Eq. 3 being less confident, but we hypothesize it’s beneficial in order to develop a robust shared multi-modal space. Finally, we experiment with optimizing both the sequence-based and the aggregation-based contrastive objective using multi-task learning (with equal importance). We notice that including the standard contrastive objective reduces recall@1 by 7 points, indicating that the two objectives result in different representation spaces, and do not work in synergy.¹¹

¹¹We did notice an improvement in aggregation-based retrieval, but the much less in magnitude than the drop in sequence-based. Experiment is done with mean-pooling, but results were the same with using a <cls> token for aggregation.

5 Conclusion

In this work we introduced a novel approach for audio-visual contrastive learning based on sequential distances, which also enables their use during inference for retrieval. We conducted experiments to investigate several distance metrics, and showed that our sequential contrastive learning using an interpolated Euclidean distance can surpass aggregation-based contrastive learning and other methods by large margins. We further showed that our method is particularly effective in a challenging out-of-distribution setting where enhanced intra-sequential discrimination capabilities are needed. Finally, we proposed a hybrid method for retrieval that provides a useful flexibility between efficiency and accuracy and opens the way for our method to be performant in large-scale retrieval scenarios. Future work will investigate the addition of the text modality in the sequential audio-visual representation space, which has the potentially to enable many multi-modal applications, like generation.

References

- [Arandjelovic and Zisserman 2017] Arandjelovic, R., and Zisserman, A. 2017. Look, Listen and Learn. In *2017 IEEE International Conference on Computer Vision (ICCV)*, 609–617. 2
- [Arandjelovic and Zisserman 2018] Arandjelovic, R., and Zisserman, A. 2018. Objects that Sound. In *Proceedings of the European Conference on Computer Vision (ECCV)*. 2
- [Baevski et al. 2020] Baevski, A.; Zhou, H.; Mohamed, A.; and Auli, M. 2020. wav2vec 2.0: A Framework for Self-supervised Learning of Speech Representations. In *Proceedings of the 34th International Conference on Neural Information Processing Systems, NIPS’20*. Red Hook, NY, USA: Curran Associates Inc. 2
- [Chen et al. 2020a] Chen, H.; Xie, W.; Vedaldi, A.; and Zisserman, A. 2020a. VGGSound: A Large-scale Audio-Visual Dataset. In *International Conference on Acoustics, Speech, and Signal Processing (ICASSP)*. 5
- [Chen et al. 2020b] Chen, T.; Kornblith, S.; Norouzi, M.; and Hinton, G. 2020b. A Simple Framework for Contrastive Learning of Visual Representations. In *Proceedings of the 37th International Conference on Machine Learning, ICML’20*. JMLR.org. 2

- [Chen et al. 2023] Chen, S.; Wu, Y.; Wang, C.; Liu, S.; Tompkins, D.; Chen, Z.; Che, W.; Yu, X.; and Wei, F. 2023. BEATs: Audio Pre-Training with Acoustic Tokenizers. In Krause, A.; Brunskill, E.; Cho, K.; Engelhardt, B.; Sabato, S.; and Scarlett, J., eds., *Proceedings of the 40th International Conference on Machine Learning*, volume 202 of *Proceedings of Machine Learning Research*, 5178–5193. PMLR. [3](#), [4](#), [5](#)
- [Cheng et al. 2023] Cheng, Z.; Xie, T.; Shi, P.; Li, C.; Nadkarni, R.; Hu, Y.; Xiong, C.; Radev, D.; Ostendorf, M.; Zettlemoyer, L.; Smith, N. A.; and Yu, T. 2023. Binding Language Models in Symbolic Languages. *ICLR*. [2](#)
- [Chi et al. 2022] Chi, Z.; Huang, S.; Dong, L.; Ma, S.; Zheng, B.; Singhal, S.; Bajaj, P.; Song, X.; Mao, X.-L.; Huang, H.; and Wei, F. 2022. XLM-E: Cross-lingual Language Model Pre-training via ELECTRA. In Muresan, S.; Nakov, P.; and Villavicencio, A., eds., *Proceedings of the 60th Annual Meeting of the Association for Computational Linguistics (Volume 1: Long Papers)*, 6170–6182. Dublin, Ireland: Association for Computational Linguistics. [4](#)
- [Chopra, Hadsell, and LeCun 2005] Chopra, S.; Hadsell, R.; and LeCun, Y. 2005. Learning a similarity metric discriminatively, with application to face verification. In *2005 IEEE Computer Society Conference on Computer Vision and Pattern Recognition (CVPR'05)*, volume 1, 539–546 vol. 1. [1](#)
- [Cuturi and Blondel 2017] Cuturi, M., and Blondel, M. 2017. Soft-DTW: a differentiable loss function for time-series. In *Proceedings of the 34th International Conference on Machine Learning - Volume 70, ICML'17*, 894–903. JMLR.org. [4](#)
- [Dosovitskiy et al. 2021] Dosovitskiy, A.; Beyer, L.; Kolesnikov, A.; Weissenborn, D.; Zhai, X.; Unterthiner, T.; Dehghani, M.; Minderer, M.; Heigold, G.; Gelly, S.; Uszkoreit, J.; and Houlsby, N. 2021. An Image is Worth 16x16 Words: Transformers for Image Recognition at Scale. In *International Conference on Learning Representations*. [3](#), [5](#)
- [Elizalde, Deshmukh, and Wang 2023] Elizalde, B.; Deshmukh, S.; and Wang, H. 2023. Natural Language Supervision for General-Purpose Audio Representations. [2](#), [4](#)
- [Frognier et al. 2015] Frognier, C.; Zhang, C.; Mobahi, H.; Araya, M.; and Poggio, T. A. 2015. Learning with a Wasserstein Loss. In Cortes, C.; Lawrence, N.; Lee, D.; Sugiyama, M.; and Garnett, R., eds., *Advances in Neural Information Processing Systems*, volume 28. Curran Associates, Inc. [2](#), [5](#)
- [Garg, Vankadari, and Milford 2021] Garg, S.; Vankadari, M.; and Milford, M. 2021. SeqMatchNet: Contrastive Learning with Sequence Matching for Place Recognition & Relocalization. In *5th Annual Conference on Robot Learning*. [2](#)
- [Gemini-Team 2023] Gemini-Team. 2023. Gemini: A Family of Highly Capable Multimodal Models. [1](#)
- [Gemmeke et al. 2017] Gemmeke, J. F.; Ellis, D. P. W.; Freedman, D.; Jansen, A.; Lawrence, W.; Moore, R. C.; Plakal, M.; and Ritter, M. 2017. Audio Set: An ontology and human-labeled dataset for audio events. In *2017 IEEE International Conference on Acoustics, Speech and Signal Processing (ICASSP)*, 776–780. [6](#)
- [Girdhar et al. 2023] Girdhar, R.; El-Nouby, A.; Liu, Z.; Singh, M.; Alwala, K. V.; Joulin, A.; and Misra, I. 2023. ImageBind: One Embedding Space To Bind Them All. In *CVPR*. [2](#), [6](#)
- [Gong et al. 2023] Gong, Y.; Rouditchenko, A.; Liu, A. H.; Harwath, D.; Karlinsky, L.; Kuehne, H.; and Glass, J. R. 2023. Contrastive Audio-Visual Masked Autoencoder. In *The Eleventh International Conference on Learning Representations*. [1](#), [2](#), [6](#)
- [Guzhov et al. 2022] Guzhov, A.; Raue, F.; Hees, J.; and Dengel, A. 2022. Audioclip: Extending Clip to Image, Text and Audio. In *ICASSP 2022 - 2022 IEEE International Conference on Acoustics, Speech and Signal Processing (ICASSP)*, 976–980. [2](#)
- [Hendrycks and Gimpel 2023] Hendrycks, D., and Gimpel, K. 2023. Gaussian error linear units (gelus). [6](#)
- [Huang et al. 2023] Huang, P.-Y.; Sharma, V.; Xu, H.; Ryali, C.; Fan, H.; Li, Y.; Li, S.-W.; Ghosh, G.; Malik, J.; and Feichtenhofer, C. 2023. MAViL: Masked Audio-Video Learners. In *Thirty-seventh Conference on Neural Information Processing Systems*. [2](#)
- [Itakura 1975] Itakura, F. 1975. Minimum prediction residual principle applied to speech recognition. *IEEE Transactions on Acoustics, Speech, and Signal Processing* 23(1):67–72. [4](#)
- [Jeong et al. 2023] Jeong, Y.; Ryoo, W.; Lee, S.; Seo, D.; Byeon, W.; Kim, S.; and Kim, J. 2023. The Power of Sound (TPoS): Audio Reactive Video Generation with Stable Diffusion. In *Proceedings of the IEEE/CVF International Conference on Computer Vision*, 7822–7832. [1](#)
- [Jia et al. 2021] Jia, C.; Yang, Y.; Xia, Y.; Chen, Y.-T.; Parekh, Z.; Pham, H.; Le, Q.; Sung, Y.-H.; Li, Z.; and Duerig, T. 2021. Scaling Up Visual and Vision-Language Representation Learning With Noisy Text Supervision. In Meila, M., and Zhang, T., eds., *Proceedings of the 38th International Conference on Machine Learning*, volume 139 of *Proceedings of Machine Learning Research*, 4904–4916. PMLR. [2](#)
- [Kalayeh et al. 2022] Kalayeh, M. M.; Ardeshtir, S.; Liu, L.; Kamath, N.; and Chandrashekar, A. 2022. On Negative Sampling for Audio-Visual Contrastive Learning from Movies. *CoRR* abs/2205.00073. [2](#)
- [Knopp and Sinkhorn 1967] Knopp, P., and Sinkhorn, R. 1967. Concerning nonnegative matrices and doubly stochastic matrices. *Pacific Journal of Mathematics* 21(2):343 – 348. [5](#)
- [Korbar, Tran, and Torresani 2018] Korbar, B.; Tran, D.; and Torresani, L. 2018. Cooperative Learning of Audio and Video Models from Self-Supervised Synchronization. In *Proceedings of the 32nd International Conference on Neural Information Processing Systems, NIPS'18*, 7774–7785. Red Hook, NY, USA: Curran Associates Inc. [1](#), [2](#)
- [Le et al. 2023] Le, P.-H.; Gong, H.; Wang, C.; Pino, J.; Lecouteux, B.; and Schwab, D. 2023. Pre-training for

- Speech Translation: CTC meets Optimal Transport. In *Proceedings of the 40th International Conference on Machine Learning, ICML'23*. JMLR.org. 5
- [Loshchilov and Hutter 2019] Loshchilov, I., and Hutter, F. 2019. Decoupled Weight Decay Regularization. In *International Conference on Learning Representations*. 6
- [Luo et al. 2023] Luo, S.; Yan, C.; Hu, C.; and Zhao, H. 2023. Diff-foley: Synchronized video-to-audio synthesis with latent diffusion models. 1
- [Ma et al. 2021a] Ma, S.; Zeng, Z.; McDuff, D.; and Song, Y. 2021a. Active Contrastive Learning of Audio-Visual Video Representations. In *International Conference on Learning Representations*. 1, 2
- [Ma et al. 2021b] Ma, S.; Zeng, Z.; McDuff, D.; and Song, Y. 2021b. Contrastive Learning of Global and Local Video Representations. In Beygelzimer, A.; Dauphin, Y.; Liang, P.; and Vaughan, J. W., eds., *Advances in Neural Information Processing Systems*. 2
- [Morgado, Misra, and Vasconcelos 2021] Morgado, P.; Misra, I.; and Vasconcelos, N. 2021. Robust Audio-Visual Instance Discrimination. In *2021 IEEE/CVF Conference on Computer Vision and Pattern Recognition (CVPR)*, 12929–12940. 2
- [Morgado, Vasconcelos, and Misra 2021] Morgado, P.; Vasconcelos, N.; and Misra, I. 2021. Audio-Visual Instance Discrimination with Cross-Modal Agreement. In *2021 IEEE/CVF Conference on Computer Vision and Pattern Recognition (CVPR)*, 12470–12481. Los Alamitos, CA, USA: IEEE Computer Society. 2
- [Owens and Efros 2018] Owens, A., and Efros, A. A. 2018. Audio-Visual Scene Analysis with Self-Supervised Multi-sensory Features. In *Computer Vision – ECCV 2018: 15th European Conference, Munich, Germany, September 8–14, 2018, Proceedings, Part VI*, 639–658. Berlin, Heidelberg: Springer-Verlag. 2
- [Peyré and Cuturi 2019] Peyré, G., and Cuturi, M. 2019. Computational Optimal Transport: With Applications to Data Science. *Foundations and Trends® in Machine Learning* 11(5-6):355–607. 5
- [Radford et al. 2021] Radford, A.; Kim, J. W.; Hallacy, C.; Ramesh, A.; Goh, G.; Agarwal, S.; Sastry, G.; Askell, A.; Mishkin, P.; Clark, J.; Krueger, G.; and Sutskever, I. 2021. Learning Transferable Visual Models From Natural Language Supervision. In Meila, M., and Zhang, T., eds., *Proceedings of the 38th International Conference on Machine Learning*, volume 139 of *Proceedings of Machine Learning Research*, 8748–8763. PMLR. 1, 2, 3, 6, 8
- [Recasens et al. 2021] Recasens, A.; Luc, P.; Alayrac, J.; Wang, L.; Strub, F.; Tallec, C.; Malinowski, M.; Patraucean, V.; Altche, F.; Valko, M.; Grill, J.; van den Oord, A.; and Zisserman, A. 2021. Broaden Your Views for Self-Supervised Video Learning. In *2021 IEEE/CVF International Conference on Computer Vision (ICCV)*, 1235–1245. Los Alamitos, CA, USA: IEEE Computer Society. 2
- [Ruan et al. 2023] Ruan, L.; Ma, Y.; Yang, H.; He, H.; Liu, B.; Fu, J.; Yuan, N. J.; Jin, Q.; and Guo, B. 2023. MM-Diffusion: Learning Multi-Modal Diffusion Models for Joint Audio and Video Generation. In *CVPR*. 1
- [Sun et al. 2023] Sun, W.; Zhang, J.; Wang, J.; Liu, Z.; Zhong, Y.; Feng, T.; Guo, Y.; Zhang, Y.; and Barnes, N. 2023. Learning Audio-Visual Source Localization via False Negative Aware Contrastive Learning. In *2023 IEEE/CVF Conference on Computer Vision and Pattern Recognition (CVPR)*, 6420–6429. Los Alamitos, CA, USA: IEEE Computer Society. 2
- [Tang et al. 2023] Tang, Z.; Yang, Z.; Zhu, C.; Zeng, M.; and Bansal, M. 2023. Any-to-Any Generation via Composable Diffusion. In *Thirty-seventh Conference on Neural Information Processing Systems*. 1
- [Tsiamas et al. 2024] Tsiamas, I.; Gállego, G. I.; Fonollosa, J. A. R.; and Costa-jussà, M. R. 2024. Pushing the Limits of Zero-shot End-to-End Speech Translation. 5
- [van den Oord, Li, and Vinyals 2019] van den Oord, A.; Li, Y.; and Vinyals, O. 2019. Representation Learning with Contrastive Predictive Coding. 1
- [Vaswani et al. 2017] Vaswani, A.; Shazeer, N.; Parmar, N.; Uszkoreit, J.; Jones, L.; Gomez, A. N.; Kaiser, L. u.; and Polosukhin, I. 2017. Attention is All you Need. In Guyon, I.; Luxburg, U. V.; Bengio, S.; Wallach, H.; Fergus, R.; Vishwanathan, S.; and Garnett, R., eds., *Advances in Neural Information Processing Systems*, volume 30. Curran Associates, Inc. 4
- [Vintsyuk 1968] Vintsyuk, T. K. 1968. Speech discrimination by dynamic programming. *IEEE Transactions on Acoustics, Speech, and Signal Processing* 4(1):52–57. 2, 4
- [Wang et al. 2023] Wang, P.; Wang, S.; Lin, J.; Bai, S.; Zhou, X.; Zhou, J.; Wang, X.; and Zhou, C. 2023. ONE-PEACE: Exploring One General Representation Model Toward Unlimited Modalities. 2
- [Wu et al. 2018] Wu, Z.; Xiong, Y.; Yu, S. X.; and Lin, D. 2018. Unsupervised Feature Learning via Non-parametric Instance Discrimination. In *2018 IEEE/CVF Conference on Computer Vision and Pattern Recognition*, 3733–3742. 6, 8
- [Wu et al. 2023a] Wu, H.-H.; Nieto, O.; Bello, J. P.; and Salamon, J. 2023a. Audio-Text Models Do Not Yet Leverage Natural Language. In *ICASSP 2023 - 2023 IEEE International Conference on Acoustics, Speech and Signal Processing (ICASSP)*, 1–5. 1
- [Wu et al. 2023b] Wu, Y.; Chen, K.; Zhang, T.; Hui, Y.; Berg-Kirkpatrick, T.; and Dubnov, S. 2023b. Large-scale Contrastive Language-Audio Pretraining with Feature Fusion and Keyword-to-Caption Augmentation. In *IEEE International Conference on Acoustics, Speech and Signal Processing, ICASSP*. 1, 2, 4
- [Xiong et al. 2020] Xiong, R.; Yang, Y.; He, D.; Zheng, K.; Zheng, S.; Xing, C.; Zhang, H.; Lan, Y.; Wang, L.; and Liu, T.-Y. 2020. On Layer Normalization in the Transformer Architecture. In *Proceedings of the 37th International Conference on Machine Learning, ICML'20*. JMLR.org. 6
- [Xu et al. 2021] Xu, H.; Ghosh, G.; Huang, P.-Y.; Okhonko, D.; Aghajanyan, A.; Metze, F.; Zettlemoyer, L.; and Feichtenhofer, C. 2021. VideoCLIP: Contrastive Pre-training

for Zero-shot Video-Text Understanding. In Moens, M.-F.; Huang, X.; Specia, L.; and Yih, S. W.-t., eds., *Proceedings of the 2021 Conference on Empirical Methods in Natural Language Processing*, 6787–6800. Online and Punta Cana, Dominican Republic: Association for Computational Linguistics. [1](#)

[Yang et al. 2023] Yang, Y.; Ma, J.; Huang, S.; Chen, L.; Lin, X.; Han, G.; and Chang, S.-F. 2023. TempCLR: Temporal Alignment Representation with Contrastive Learning. In *The Eleventh International Conference on Learning Representations*. [2](#)

[Zhang, Li, and Bing 2023] Zhang, H.; Li, X.; and Bing, L. 2023. Video-LLaMA: An Instruction-tuned Audio-Visual Language Model for Video Understanding. In Feng, Y., and Lefever, E., eds., *Proceedings of the 2023 Conference on Empirical Methods in Natural Language Processing: System Demonstrations*, 543–553. Singapore: Association for Computational Linguistics. [1](#)

[Zhao et al. 2018] Zhao, H.; Gan, C.; Rouditchenko, A.; Vondrick, C.; McDermott, J.; and Torralba, A. 2018. The Sound of Pixels. In *The European Conference on Computer Vision (ECCV)*. [2](#), [5](#)

[Zhao et al. 2019] Zhao, H.; Gan, C.; Ma, W.-C.; and Torralba, A. 2019. The sound of motions. In *Proceedings of the IEEE International Conference on Computer Vision*, 1735–1744. [5](#)